

Astroparticle Physics

Student presentations:

28.02.2019 Air showers - Matthews Heitler model	NN
28.02.2019 Radio detection of air showers	NN
07.03.2019 Cosmic ray anisotropy at TeV energies, IceCube/Top, HAWK	Gerfen, Niek
07.03.2019 The knee in the energy spectrum of cosmic rays	Yagnik, Jwalant
11.04.2019 Detectors for ultra-high-energy cosmic rays, Auger, TA	Athanasiadou, Sofia
11.04.2019 Proton-air cross section measured by the AUger observatory	Wijte, Thomas
18.04.2019 GZK effect and the end of the cosmic-ray spectrum	Willemsen, Patrick
18.04.2019 Cosmic ray mass composition at the highest energies, Auger, TA	Carrasco I Brossa, Marta
09.05.2019 Cosmic-ray anisotropy at high energies, Auger, TA	Leenders, Olaf
09.05.2019 IceCube neutrino astronomy	de Boone, Eric Teunis
16.05.2019 KM3NeT project, ARCA+ORCA	Bouma, Ronald
16.05.2019 H.E.S.S. TeV gamma-ray astronomy galactic center emission	Khakurdikar, Abha
23.05.2019 H.E.S.S. gamma-ray astronomy galactic plane survey	Remeijn, Jur
23.05.2019 Cherenkov telescope array - CTA	Traykov, Viktor
06.06.2019 XENON dark matter search	Mink, Maaïke
06.06.2019 LIGO + VIRGO gravitational waves	Terwel, Jacco

<http://particle.astro.ru.nl/goto.html?astropart1819>

Astroparticle Physics

Lectures:

- 05.02.2019 [1. Historical introduction, basic properties of cosmic rays](#)
- 07.02.2019 [2. Hadronic interactions and accelerator data](#)
- 19.02.2019 3. Cascade equations
- 21.02.2019 4. Electromagnetic cascades
- 26.02.2019 5. Extensive air showers
- 05.03.2019 6. High energy cosmic rays and the knee in the energy spectrum of cosmic rays
- 05.03.2019 7. Acceleration, astrophysical accelerators and beam dumps
- 09.04.2019 8. Extragalactic propagation of cosmic rays
- 23.04.2019 9. Ultra high energy cosmic rays
- 07.05.2019 10. Astrophysical gamma rays and neutrinos
- 14.05.2019 11. Neutrino astronomy
- 21.05.2019 12. Gamma-ray astronomy
- 28.05.2019 13. Dark matter detectors
- 04.06.2019 14. Gravitational wave detectors

<http://particle.astro.ru.nl/goto.html?astropart1819>

lecture 3

Cascade equations

Gaisser chapter 5

- 5 **Cascade equations**
 - 5.1 Basic equation and boundary conditions
 - 5.2 Boundary conditions
 - 5.3 Energy loss by charged particles
 - 5.4 Electrons, positrons and photons
 - 5.5 Nucleons in the atmosphere
 - 5.6 Hadrons in the atmosphere
 - 5.7 The atmosphere
 - 5.8 Meson fluxes

In the next few chapters we will discuss cosmic ray cascades specifically in the atmosphere of the Earth. Many of the basic ideas and results apply also to many other settings and problems of interest that will be discussed later. These include particle production in stellar atmospheres and in outflows from active galaxies and astrophysical explosions, as well as in propagation through the interstellar medium.

5.1 Basic equation and boundary conditions

The linear development of a cascade of particles in the atmosphere can be described by a system of equations of the form

$$\frac{dN_i(E_i, X)}{dX} = -\frac{N_i(E_i, X)}{\lambda_i} - \frac{N_i(E_i, X)}{d_i} + \sum_{j=i}^J \int_E^{\infty} \frac{F_{ji}(E_i, E_j)}{E_i} \frac{N_j(E_j, X)}{\lambda_j} dE_j. \quad (5.1)$$

Here, $N_i(E_i, X)dE_i$ is the flux of particles of type i at slant depth X in the atmosphere with energies in the interval E to $E + dE$. Note that X is measured from the top of the atmosphere downward along the direction of the particle that initiated the cascade, as shown in Figure 5.1. The probability that a particle of type j interacts in traversing an infinitesimal element of the atmosphere is $dX/\lambda_j(E_j)$, where λ_j is the interaction length in air of particles of type j . Similarly, $dX/d_j(E_j)$ is the probability that a particle of type j decays in dX . All three quantities X , λ_j and d_j must be expressed in consistent units, and we use g/cm^2 . Energy loss by ionization is not included in Eq. 5.1 because it is not important for hadrons in the atmosphere or for high-energy electrons.

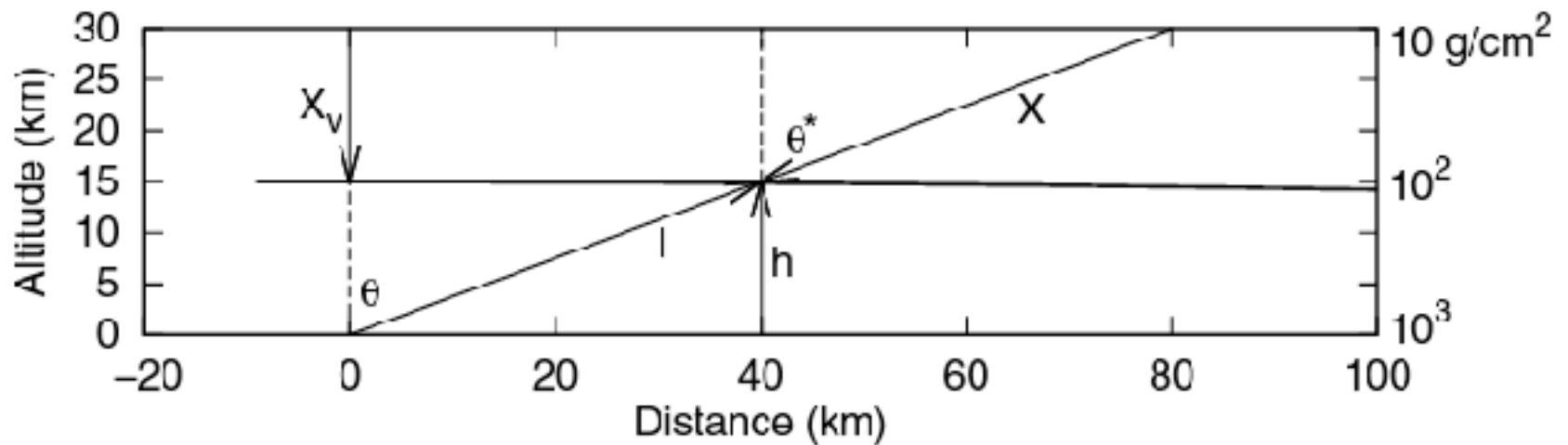


Figure 5.1 Definition of variables to describe the atmosphere. X is the slant depth, θ^* is the local zenith angle in the atmosphere at slant depth X , and h is the local vertical altitude. Vertical depth (g/cm^2) is indicated on the right. The zenith angle θ at the detector is larger than θ^* because of curvature of the Earth.

Interaction length and decay length depend on density of the medium in different ways. A characteristic length in g/cm^2 is obtained by multiplying the corresponding length in cm by the density. Thus

$$\lambda_j = \ell_j \rho = \frac{\rho}{n_A \sigma_j^{\text{air}}} = \frac{A m_p}{\sigma_j^{\text{air}}}, \quad (5.2)$$

where $\rho(h)$ is the density of the atmosphere at altitude h and n_A is the corresponding local number density of nuclei of mean mass A in the atmosphere. For a derivation of Eq. 5.2, see Appendix A.3. The dependence on density cancels out of the interaction length when expressed in g/cm^2 . The decay length, however, is proportional to density,

$$d_j = \rho \gamma c \tau_j, \quad (5.3)$$

where γ is the Lorentz factor of a particle with rest lifetime τ_j .

The function $F_{ji}(E_i, E_j)$ in Eq. 5.1 is the dimensionless particle yield that follows from the inclusive cross section (integrated over transverse momentum) for a particle of energy E_j to collide with an air nucleus and produce an outgoing particle i with energy $E_i < E_j$. In general, we define

$$F_{ji}(E_i, E_j) \equiv E_i \frac{1}{\sigma_j^{\text{air}}} \frac{d\sigma_{j \text{ air} \rightarrow i}}{dE_i} = E_i \frac{dn_i(E_i, E_j)}{dE_i}, \quad (5.4)$$

where dn_i is the number of particles of type i produced on average in the energy bin dE_i around E_i per collision of an incident particle of type j . All quantities in Eq. 5.4 are defined in the lab system. The relation to center-of-mass quantities can be derived from the definitions in Table 4.1. From Eq. 4.15 it follows that for energetic secondaries, i.e. those with $E_c \gg m_{T,c}$

$$E_c/E_a = x_L \approx x^*. \quad (5.5)$$

(We always define CMS as a projectile on a target *nucleon* even when that nucleon is bound in a nucleus, because nuclear binding energies will usually be much lower than energies of interest in cosmic ray problems we consider.)

Some insight into how the cascade equation 5.1 works may be gained by calculating the spectrum of pions $\Pi(E_\pi)$ produced by a power-law spectrum of nucleons ($N(E) = K E^{-(\gamma+1)}$) passing through a thin target of thickness dX given in g/cm^2 . We assume the scaling approximation in which the transfer function F_{ji} depends only on the ratio of the energy of the produced particle to the energy of the beam particle (x_L as defined in Eq. 5.5). Then

$$\begin{aligned} \frac{d\Pi(E_\pi)}{dX} &= \int_{E_\pi}^{\infty} \frac{F_{N\pi}(x_L)}{E_\pi} \frac{N(E_N)}{\lambda_N} dE_N \\ &= \frac{1}{\lambda_N} \int_0^1 N(E_\pi/x_L) F_{N\pi}(x_L) \frac{dx_L}{x_L^2} \\ &= \frac{K}{\lambda_N} \int_0^1 \left(\frac{x_L}{E_\pi}\right)^{\gamma+1} F_{N\pi}(x_L) \frac{dx_L}{x_L^2} \\ &= \frac{N(E_\pi)}{\lambda_N} \int_0^1 x_L^{\gamma-1} F_{N\pi}(x_L) dx_L \equiv \frac{N(E_\pi)}{\lambda_N} Z_{N\pi}. \end{aligned} \quad (5.6)$$

The *spectrum-weighted moment*

$$Z_{N\pi} = \int_0^1 x_L^{\gamma-1} F_{N\pi}(x_L) dx_L = \int_0^1 x_L^{\gamma} \frac{dn_\pi}{dx_L} dx_L \quad (5.7)$$

characterizes the physics of pion production by a spectrum of nucleons. An important implication of Eq. 5.6 is that, in the scaling approximation, the production spectrum of the secondaries has the same power as the beam spectrum. Spectrum-weighted moments are discussed further in Section 5.5 of this chapter.

5.2 Boundary conditions

We will need solutions of the cascade equation 5.1 subject to two physically important boundary conditions that correspond to two quite different types of experiments. The boundary conditions are

$$N(E, 0) = N_0(E) = \frac{dN}{dE} \approx 1.7 E^{-2.7} \frac{\text{nucleons}}{\text{cm}^2 \text{ sr s GeV}/A} \quad (5.8)$$

*power-law
spectrum*

and

$$N(E, 0) = A \delta\left(E - \frac{E_0}{A}\right) \delta(t - t_0), \quad (5.9)$$

*air
showers*

where A here is the mass number of an incident nucleus. Eq. 5.8 is relevant for a detector that simply measures the rate at which particles of a given type pass through. The explicit power law approximation is based on data with primary energy less than a TeV, but it is useful as a guide up to a PeV. Eq. 5.9 is the boundary condition relevant for an air shower experiment that traces the development of a cascade through the atmosphere. An example is an array of detectors on the ground with a fast-timing capability that can be triggered to measure the coincident, extended shower front initiated at the top of the atmosphere by a single particle. In the case of a ground array, the primary particle has to have sufficient energy to give a measurable cascade at the surface of the Earth. Cherenkov and fluorescence detectors can trace the development of showers through the atmosphere.

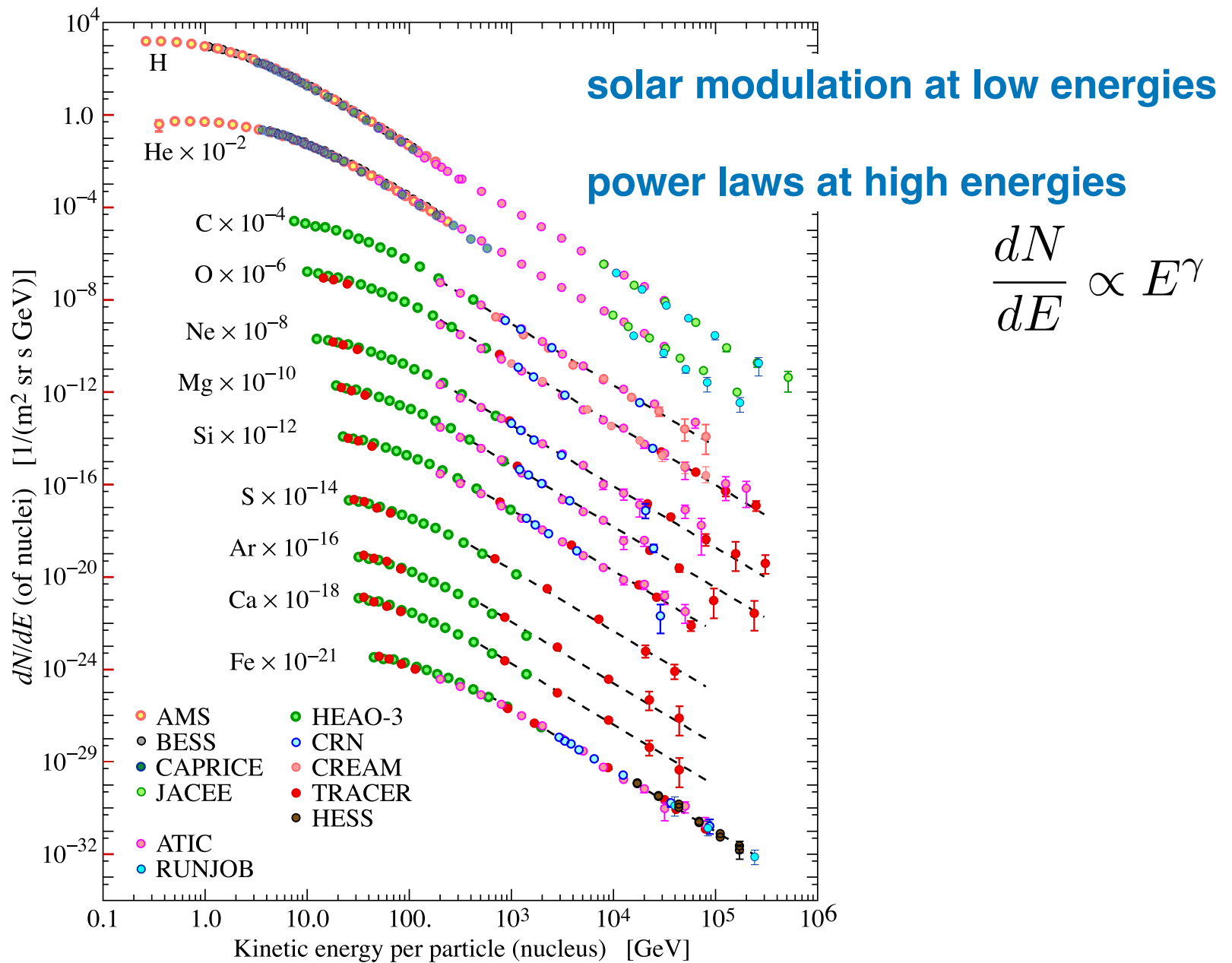


Figure 24.1: Major components of the primary cosmic radiation from Refs. [1–12]. The figure was created by P. Boyle and D. Muller. Color version at end of book.

5.3 Energy loss by charged particles

Charged particles lose energy by ionizing the medium through which they propagate and by interacting with nuclei to produce secondary radiation. Losses due to ionization vary slowly with energy, while radiative losses increase in proportion to energy. This leads to the simple approximate form,

$$\frac{dE}{dX} = -\alpha - E/\xi, \quad (5.10)$$

where E is the energy of the particle, dX is the amount of matter traversed, and the energy loss parameters α (MeV/g/cm²) and ξ (g/cm²) vary slowly with energy. The critical energy E_c can be defined as the energy at which radiative losses equal ionization losses. Then

$$E_c = \alpha \times \xi. \quad (5.11)$$

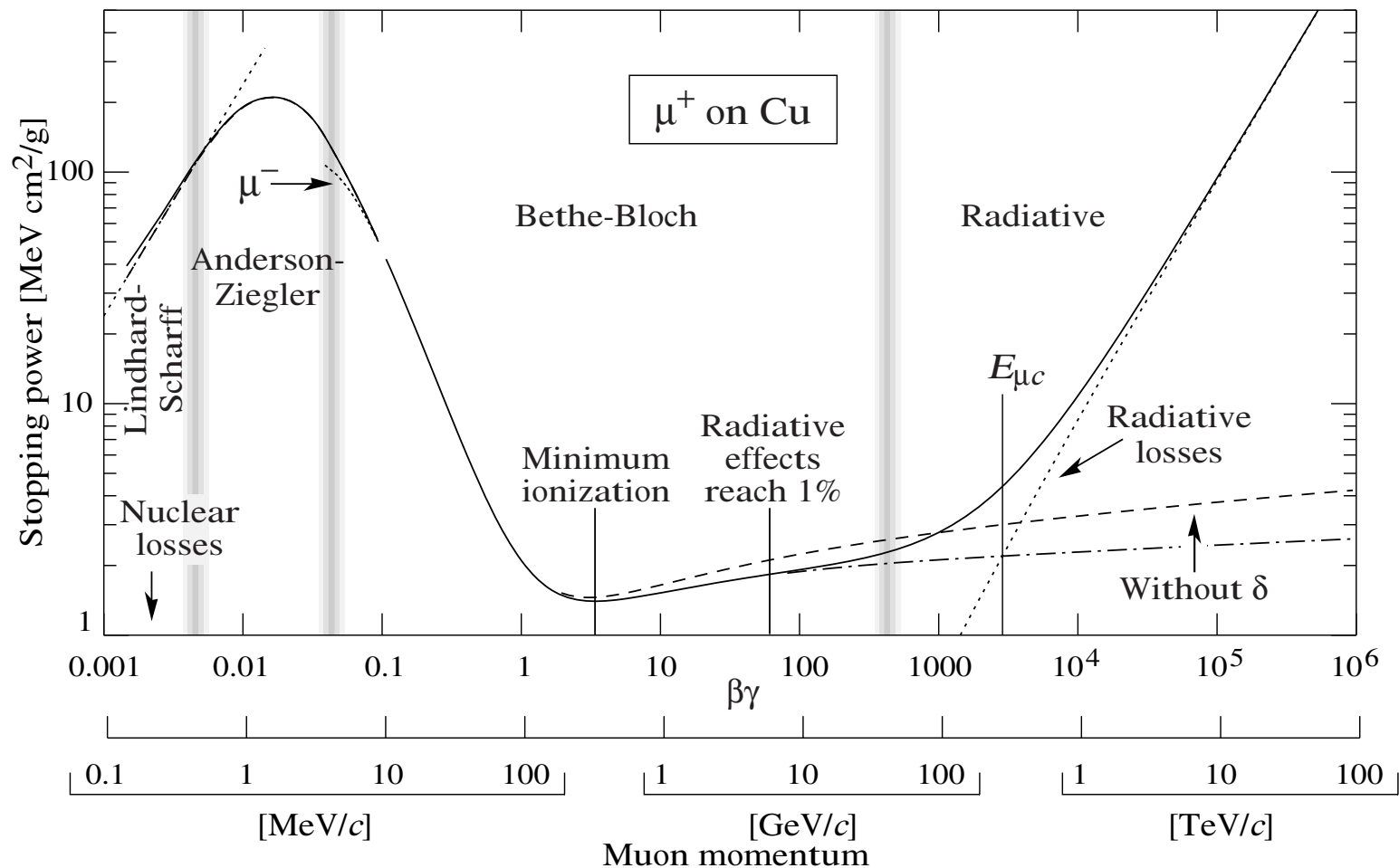


Fig. 27.1: Stopping power ($= \langle -dE/dx \rangle$) for positive muons in copper as a function of $\beta\gamma = p/Mc$ over nine orders of magnitude in momentum (12 orders of magnitude in kinetic energy). Solid curves indicate the total stopping power. Data below the break at $\beta\gamma \approx 0.1$ are taken from ICRU 49 [4], and data at higher energies are from Ref. 5. Vertical bands indicate boundaries between different approximations discussed in the text. The short dotted lines labeled “ μ^- ” illustrate the “Barkas effect,” the dependence of stopping power on projectile charge at very low energies [6].

The parameters in Eq. 5.10, and hence the phenomenology of energy loss, depend strongly on the identity of the particle and, to a lesser extent, on the properties of the medium in which they propagate.¹ In particular, bremsstrahlung losses, which involve transverse acceleration of the propagating particle, are proportional to $r_e^2 \times (m_e/M)^2$, where $r_e = e^2/(m_e c^2) \approx 2.818$ fm is the classical radius of the electron and m_e/M is the ratio of the mass of the electron to the mass of the radiating particle. Bremsstrahlung is the dominant radiative loss process for electrons and dominates above $E_c(e) \approx 87$ MeV in the atmosphere. The factor $(m_e/m_\mu)^2$ suppresses bremsstrahlung for muons of mass $m_\mu = 106$ MeV by more than four orders of magnitude. Muons also lose energy by photon-mediated fragmentation of nuclei, including pion production, and by direct pair production ($\mu + A \rightarrow \mu + A + e^+ + e^-$). These have an effect comparable to that of bremsstrahlung. As a consequence, the critical energy for muons is $E_c(\mu) \sim 500$ GeV. We will discuss energy loss by muons in more detail in Chapter 8 in connection with its consequences for observation of muons underground.

For $E \gg E_c$, the solution of Eq. 5.10 for a particle injected at $X = 0$ with an initial energy E_0 is

$$L(X) = E_0 \times \exp\left[\frac{-X}{\xi}\right]. \quad (5.12)$$

For electrons, ξ is called the radiation length, often represented by $\xi = X_0$. Its value for electrons is 63 g/cm² in hydrogen, 36 g/cm² in water, 37 g/cm² in air, 22 g/cm² in silicon and 13.8 g/cm² in iron.

Electrons, positrons and photons

The basic high-energy processes that make up an electromagnetic cascade are pair production and bremsstrahlung. The basic formulas are due to Hans Bethe (1934) [189]. The shower energy is eventually dissipated by ionization of the medium by all the electrons and positrons in the cascade. As long as we consider particles with energies large compared to the critical energy, however, collision losses, and also Compton scattering, can be neglected in calculating the development of the cascade. Since both pair production and bremsstrahlung occur in the field of an atomic nucleus, the processes will be screened by the atomic electrons for impact parameters larger than the radius of the atom.

On the Stopping of Fast Particles and on the Creation of Positive Electrons

By H. BETHE, Manchester, and W. HEITLER, Bristol

(Communicated by P. A. M. DIRAC, F.R.S.—Received February 27, 1934)

Introduction

The stopping power of matter for fast particles is at present believed to be due to three different processes: (1) the ionization; (2) the nuclear scattering; (3) the emission of radiation under the influence of the electric field of a nucleus. The first two processes have been treated in quantum mechanics by Bethe,[†] Møller,[‡] and Bloch[§] in a very satisfactory way. A provisional estimation of the order of magnitude to be expected in the third process has been given by Heitler.^{||} The result obtained was that the cross-section ϕ for the energy loss by radiation for very fast particles (if the primary energy $E_0 \gg mc^2$) is of the order

$$\phi \approx \frac{Z^2}{137} \left(\frac{e^2}{mc^2} \right)^2, \quad (1)$$

where Z is the nuclear charge.

It is the aim of the present paper to discuss in greater detail the rate of loss of energy by this third process and its dependence on the primary energy; in particular we shall consider the effect of *screening*. The results obtained for very high energies ($> 137 mc^2$) seem to be in disagreement with experiments made by Anderson (*cf.* § 7).

By an exactly similar calculation another process can be studied, namely, the "twin birth" of a positive and negative electron due to a light quantum in the presence of a nucleus. This process is the converse of the scattering of an electron with loss of radiation, if the final state has *negative* energy. The results are in exact agreement with recent measurements for γ -rays of 3-10 mc^2 . A provisional estimate of the probability of this process has been given by Fieser and Oppenheimer,[¶] who also obtain for the cross-section a quantity of the order of magnitude given by equation (1).

[†] 'Ann. Physik,' vol. 5, p. 325 (1930); 'Z. Physik,' vol. 76, p. 293 (1932).

[‡] 'Ann. Physik,' vol. 14, p. 681 (1932).

[§] 'Z. Physik,' vol. 81, p. 369 (1933); 'Ann. Physik,' vol. 16, p. 235 (1933).

^{||} 'Z. Physik,' vol. 84, p. 145 (1933). Referred to later as L.

[¶] 'Phys. Rev.,' vol. 44, p. 68 (1933).

H. Bethe and W. Heitler
Proceedings of the Royal Society of London. Series A, Containing Papers of a Mathematical and Physical Character
 Vol. 146, No. 856 (Aug. 1, 1934), pp. 83-112

The probability for an electron of energy E to radiate a photon of energy $W = vE$ in traversing $dt = dX/X_0$ of atmosphere is $\phi(E, v)dt dv$, with

$$\phi(E, v) \rightarrow \phi(v) = v + \frac{1-v}{v} \left(\frac{4}{3} + 2b \right). \quad (5.13)$$

Here we use the conventional notation of electromagnetic cascade theory and scale the distance in units of the radiation length, X_0 . The parameter b in Eq. 5.13 is

$$b \equiv (18 \ln[183/Z^{1/3}])^{-1} \approx 0.0122. \quad (5.14)$$

The energy loss rate due to bremsstrahlung is therefore

$$\frac{dE}{dX} = -\frac{1}{X_0} \int_0^1 (vE) \phi(v) dv = -\frac{1}{X_0} E \times (1 + b) \approx -\frac{E}{X_0}, \quad (5.15)$$

which has the expected form of Eq. 5.12.

The corresponding probability for a photon to produce a pair in which the positron, say, has energy $E = uW$ is $\psi(W, u)dtdu$. In approximation A,

$$\psi(W, u) \rightarrow \psi(u) = \frac{2}{3} - \frac{b}{2} + \left(\frac{4}{3} + 2b\right) \left(u - \frac{1}{2}\right)^2. \quad (5.16)$$

Unlike the case for bremsstrahlung, which has the characteristic infrared divergence, the pair production probability can be integrated to get the total probability for pair production per unit radiation length. It is

$$1/\lambda_{\text{pair}} = \int_0^1 \psi(u) du = 7/9 - b/3 \approx 7/9. \quad (5.17)$$

From Eq. 5.2 the pair production cross section per target air nucleus is therefore

$$\sigma_{\gamma \rightarrow e^+e^-} \approx \frac{7}{9} \frac{A}{N_A X_0} \approx 500 \text{ mb}. \quad (5.18)$$

The cross section for bremsstrahlung,

$$\frac{1}{\lambda_{\text{brems}}} = \int_0^1 \phi(v) dv, \quad (5.19)$$

is logarithmically divergent at $v \rightarrow 0$. This infrared divergence requires special care when the distributions (5.13) and (5.15) are used as the basis of a Monte Carlo calculation. Basically, a simulation consists of choosing randomly the distance a photon (or electron) propagates from an exponential distribution with characteristic length λ_{pair} (or λ_{brems}), then splitting the energy randomly according to the distribution 5.16 for pair production or 5.13 for bremsstrahlung. A cutoff procedure must be introduced for bremsstrahlung to handle the infrared divergence. The procedure must be tailored to the application, but basically it consists of using a cutoff, v_{min} , chosen so that $v_{\text{min}} E_0 \ll E_{\text{th}}$, where E_{th} is the lowest energy of interest in the problem.² At low energies, incomplete screening, energy loss by ionization and Coulomb scattering must also be included. Standard packages for calculating electromagnetic cascades in a user-defined, complex medium are the programs GEANT [191], EGS [192] and FLUKA [193].

5.4.1 Cascade equations

The coupled equations for electromagnetic cascades are an instance of Eq. 5.1.

They are
number of photons at depth t and

$$\frac{d\gamma}{dt} = -\frac{\gamma(W, t)}{\lambda_{\text{pair}}} + \int_W^\infty \pi(E', t) \frac{dn_{e \rightarrow \gamma}}{dW dt} dE' \quad (5.20)$$

number of e^\pm at depth t

$$\begin{aligned} \frac{d\pi}{dt} = & -\frac{\pi(E, t)}{\lambda_{\text{brems}}} + \int_E^\infty \pi(E', t) \frac{dn_{e \rightarrow e}}{dE dt} dE' \\ & + 2 \int_E^\infty \gamma(W', t) \frac{dn_{\gamma \rightarrow e}}{dE dt} dW', \end{aligned} \quad (5.21)$$

where $\gamma(W, t)dW$ is the number of photons in dW at depth t and $\pi(E, t)dE$ is the number of e^\pm in dE at depth t . For energies that are large compared to the critical energy, collisional losses and Coulomb scattering can be neglected and the scaling functions 5.13 and 5.16 can be used. This is Approximation A.

This is Approximation A. With the

identifications,

$$E' \frac{dn_{e \rightarrow \gamma}}{dW dt} = \phi\left(\frac{W}{E'}\right), \quad (5.22)$$

$$W' \frac{dn_{\gamma \rightarrow e}}{dE dt} = \psi\left(\frac{E}{W'}\right) \quad (5.23)$$

and

$$E' \frac{dn_{e \rightarrow e}}{dE dt} = \phi\left(1 - \frac{E}{E'}\right), \quad (5.24)$$

the cascade equations 5.20 and 5.21 can be written in scaling form:

$$\textit{photons} \quad \frac{d\gamma}{dt} = -\frac{\gamma}{\lambda_{\text{pair}}} + \int_0^1 \pi\left(\frac{W}{v}, t\right) \phi(v) \frac{dv}{v} \quad (5.25)$$

and

$$e^{+-} \quad \frac{d\pi}{dt} = -\frac{\pi}{\lambda_{\text{brems}}} + \int_0^1 \pi\left(\frac{E}{1-v}, t\right) \phi(v) \frac{dv}{1-v} + 2 \int_0^1 \gamma\left(\frac{E}{u}, t\right) \psi(u) \frac{du}{u}. \quad (5.26)$$

The first two terms on the right side of Eq. 5.26 must be combined (using the relation 5.19) to remove the infrared divergence at $v \rightarrow 0$.

5.4.2 Power law solutions

By direct substitution it is straightforward to show that Eqs. 5.25 and 5.26 have solutions of the form

$$\gamma(W, t) = f_\gamma(t) W^{-(s+1)} \quad \text{and} \quad \pi(E, t) = f_\pi(t) E^{-(s+1)} \quad (5.27)$$

in which the dependence on depth t and energy factorize. Substituting these trial forms into Eqs. 5.20 and 5.21 and changing to scaled energy variables gives

$$f'_\gamma(t) = -f_\gamma(t)/\lambda_{\text{pair}} + f_\pi(t) \int_0^1 v^s \phi(v) dv \quad (5.28)$$

and

$$f'_\pi(t) = -f_\pi(t) \int_0^1 [1 - (1-v)^s] \phi(v) dv + f_\gamma(t) 2 \int_0^1 u^s \psi(u) du. \quad (5.29)$$

Because of the scaling form of the differential cross sections of Eq. 5.23, which depend only on the ratio of the energy of the produced particle to that of the incident particle, the energy dependence cancels out and we are left with ordinary differential equations for the dependence on depth. Note also how the infrared divergence cancels in the first term on the right-hand side of Eq. 5.29.

The integrals in Eqs. 5.28 and 5.29 are spectrum-weighted moments of the cross sections for bremsstrahlung and pair production. Analogous quantities called *Z-factors* appear in the solutions of the cascade equations for hadrons, as discussed later in this chapter.³

Table 5.1 gives some values for the spectrum-weighted moments and other parameters of electromagnetic cascade theory in the conventional notation of [194].

Table 5.1 *Definitions used in cascade theory*

Quantity	Conventional notation	$s = 1.0$	$s = 1.7$
$1/\lambda_{\text{pair}}$	$\sigma_0 \approx 7/9$	0.774	0.774
$\int_0^1 [1 - (1 - v)^s] \phi(v) dv$	$A(s)$	1.0135	1.412
$2 \int_0^1 u^s \psi(u) du$	$B(s) (= Z_{\gamma \rightarrow e})$	0.7733	0.5842
$\int_0^1 v^s \phi(v) dv$	$C(s) (= Z_{e \rightarrow \gamma})$	1.0135	0.5666
root of Eq. 5.33	$\lambda_1(s)$	0.0	-0.435
root of Eq. 5.33	$\lambda_2(s)$	-1.7868	-1.751

Table 5.1 gives some values for the spectrum-weighted moments and other parameters of electromagnetic cascade theory in the conventional notation of [194]. In terms of these definitions, Eqs. 5.28 and 5.29 may be rewritten as

$$\left[\frac{d}{dt} + \sigma_0 \right] f_\gamma(t) - C(s) f_\pi(t) = 0 \quad (5.30)$$

and

$$\left[\frac{d}{dt} + A(s) \right] f_\pi(t) - B(s) f_\gamma(t) = 0. \quad (5.31)$$

By solving Eq. 5.30 for f_π and substituting the result into Eq. 5.31 we get a second order differential equation for f_π . Similarly, substituting f_γ from Eq. 5.31 into Eq. 5.30, we get the equation for f_γ . Both $f_\pi(t)$ and $f_\gamma(t)$ satisfy the same second order differential equation,

$$f'' + (A + \sigma_0) f' + (A\sigma_0 - BC) f = 0, \quad (5.32)$$

which has elementary solutions of the form $f \propto \exp(\lambda t)$, where $\lambda(s)$ satisfies the quadratic equation obtained by substitution of the exponential form into Eq. 5.32,

$$\lambda^2 + (A + \sigma_0) \lambda + (A\sigma_0 - BC) = 0. \quad (5.33)$$

The roots of Eq. 5.33 are

$$2\lambda_1(s) = -[A(s) + \sigma_0] + \{[A(s) - \sigma_0]^2 + 4B(s)C(s)\}^{\frac{1}{2}} \quad (5.34)$$

and

$$2\lambda_2(s) = -[A(s) + \sigma_0] - \{[A(s) - \sigma_0]^2 + 4B(s)C(s)\}^{\frac{1}{2}}. \quad (5.35)$$

The solutions, $f_\gamma(t)$ and $f_\pi(t)$, are linear combinations of the elementary solutions $\exp[\lambda_1 t]$ and $\exp[\lambda_2 t]$ appropriate for the boundary conditions at injection. For example, for a power-law distribution of injected photons with $\gamma(W, 0) = f_\gamma(0)W^{-(s+1)}$ at the top of the atmosphere,

$$f_\pi(t) = \frac{Bf_\gamma(0)}{\lambda_1 - \lambda_2} \{e^{\lambda_1 t} - e^{\lambda_2 t}\} \quad (5.36)$$

and

$$f_\gamma(t) = \frac{f_\gamma(0)}{\lambda_1 - \lambda_2} \{(A + \lambda_1)e^{\lambda_1 t} - (A + \lambda_2)e^{\lambda_2 t}\}. \quad (5.37)$$

Thus, for a spectrum of injected photons with integral spectral index γ and no injected electrons, the differential spectrum of photons plus electrons and positrons at depth t is

$$\frac{dN_{\gamma+e^\pm}}{dE} = \frac{f_\gamma(0)}{\lambda_1 - \lambda_2} E^{-(\gamma+1)} \{(A + B + \lambda_1)e^{\lambda_1 t} - (A + B + \lambda_2)e^{\lambda_2 t}\}. \quad (5.38)$$

For depths greater than one radiation length, only the first term is important. With the numerical values from Table 5.1 for $\gamma = s = 1.7$,

$$\frac{dN_{\gamma-e^\pm}}{dE} \sim 1.18 f_\gamma(0) E^{-2.7} e^{-X/85}, \quad (5.39)$$

where the depth in Eq. 5.39 is expressed in g/cm^2 . Note that for $s = \gamma = 1$, $\lambda_1(s = 1) = 0$ and there is no attenuation. This is an unsustainable situation because an input spectrum with an E^{-1} integral spectrum has a logarithmically divergent energy content.

We will return to properties of solutions of the electromagnetic cascade equation for δ -function boundary conditions in connection with the discussion of air showers in Chapter 15. *see next lecture, electromagnetic cascades*

5.5 Nucleons in the atmosphere

The simplest version of Eq. 5.1 that corresponds to a physically realistic (and historically important) measurement is an approximate form for the propagation of nucleons

$$\frac{dN(E, X)}{dX} = -\frac{N(E, X)}{\lambda_N(E)} + \int_L^\infty \frac{N(E', X)}{\lambda_N(E')} F_{NN}(E, E') \frac{dE'}{E}. \quad (5.40)$$

Here $N(E, X)dE$ is the flux of nucleons (neutrons plus protons) at depth X in the atmosphere. As in the electromagnetic case, it is possible to find *elementary solutions* in which the dependence on energy and depth factorizes: $N(E, X) = G(E)g(X)$. Substitution of the factorized form into Eq. 5.40, together with a change of variable from E' to $x_L = E/E'$, gives

$$G g' = -\frac{G g}{\lambda_N} + g \int_0^1 \frac{G(E/x_L) F_{NN}(x_L, E)}{\lambda_N(E/x_L)} \frac{dx_L}{x_L^2}. \quad (5.41)$$

This separates to

$$\frac{g'}{g} = -\frac{1}{\lambda_N(E)} + \frac{1}{G(E)} \int_0^1 \frac{G(E/x_L) F_{NN}(x_L, E)}{\lambda_N(E/x_L)} \frac{dx_L}{x_L^2}. \quad (5.42)$$

If we define a separation constant $-1/\Lambda$, the solution of the differential equation for $g(X)$ is written

$$g(X) = g(0) \exp(-X/\Lambda). \quad (5.43)$$

This elementary solution has the property that the flux attenuates exponentially through the atmosphere with attenuation length Λ while preserving an energy spectrum $G(E)$ that is independent of depth. In general, because of the complicated

constraint placed on $G(E)$ by Eq. 5.41, the elementary solution does not correspond to either of the physically significant boundary conditions, Eqs. 5.8 or 5.9. We show next, however, that it is approximately valid for the power law boundary condition (Eq. 5.8).

5.5.1 Approximation A for hadrons

In electromagnetic cascade theory the form of the equations in which energy loss by ionization is neglected, the radiation length is independent of energy, and the inclusive cross sections for pair production and bremsstrahlung scale are called Approximation A. It is valid for large energy. We have just seen in the previous section how these conditions on the cross sections allow power-law solutions.

For hadrons the analogous approximations are

$$\lambda_N(E) \rightarrow \lambda_N = \text{constant} \quad (5.44)$$

and

$$F_{NN}(x_L, E) \rightarrow F_{NN}(x_L). \quad (5.45)$$

In fact, the interaction cross section (and hence λ_N) varies slowly with energy, and the assumption of hadronic scaling (Eq. 5.45) is also violated. These energy dependences are mild enough in practice, however, that the solutions in Approximation A are useful over limited energy ranges, at least as a guide to more detailed results.

This is nice because, to a good approximation, the power-law solutions of approximation A for hadrons satisfy the boundary condition imposed by the primary cosmic ray spectrum. For nucleons, as approximated by Eq. 5.40, the solution is

$$N(E, X) = g(0) e^{-X/\Lambda} E^{-(\gamma+1)}, \quad (5.46)$$

where the attenuation length is given by

$$\frac{1}{\Lambda} = \frac{1}{\lambda_N} \left[1 - \int_0^1 (x_L)^\gamma {}^1F_{NN}(x_L) dx_L \right] = \frac{1 - Z_{NN}}{\lambda_N} \quad (5.47)$$

and $-\gamma \cong -1.7$ is the power of the integral energy spectrum. The quantity Z_{NN} is the spectrum-weighted moment for a nucleon to produce a nucleon. From Eq. 5.46 we see that nucleon fluxes in the atmosphere have the same energy spectrum as the primary cosmic rays to the extent that scaling is valid. This connection between scaling for hadronic cross sections and the spectrum of hadrons in the atmosphere was recognized already by Heitler & Jánossy in 1949 [195, 196]. Like Feynman 20 years later [140], they motivated the scaling form for pion production by nucleons by analogy with bremsstrahlung of photons by electrons.

In general, the spectrum-weighted moments of the inclusive cross sections $j \rightarrow i$,

$$Z_{ji} \equiv \int_0^1 (x_L)^{\gamma-1} F_{ji}(x_L) dx_L, \quad (5.48)$$

determine the uncorrelated fluxes of energetic particles in the atmosphere [197, 198]. For $\gamma = 1$, it follows from Eq. 5.4 that $Z_{ji}(1)$ is simply the average fraction of the interaction energy that goes into particles of type i in interactions of particles of type j . For $\gamma > 1$ the contribution to the moment from $x_L \rightarrow 0$ vanishes. Thus, for a steep primary spectrum, the uncorrelated fluxes depend on the behavior of the inclusive cross sections only in the forward fragmentation region ($x^* > 0$ in Eqs. 4.15 and 5.5). This is why the μ^1/μ ratio remains large and greater than 1, which we will discuss in Chapter 6. It is also why Approximation A remains useful for uncorrelated fluxes of energetic particles, because hadronic scaling (Eq. 5.45) is more nearly valid in the fragmentation regions than elsewhere.

For later reference, we give here a table (Table 5.2) of spectrum-weighted moments.⁴ This table is analogous to the Table 5.1 for electrons and photons. The Z -factors from Ref. [199] are tabulated for $\gamma = 1$, $\gamma = 1.7$ and $\gamma = 2.0$. For comparison, we also show the Z -factors at $\gamma = 1.7$ for the first edition of this book [200] and for a new version of Sibyll [155]. Since the primary spectrum is not a perfect power-law over the whole energy region, it is also important to see how the Z -factors depend on spectral index. This is shown in Figure 5.2 for integral spectral indexes between $\gamma = 1$ (momentum fraction) and $\gamma = 2.4$ (above the knee).

Table 5.2 *Spectrum-weighted moments at 1 TeV*

Index	$\gamma = 1$ Ref. [199]	$\gamma = 1.7$	$\gamma = 2.0$	$\gamma = 1.7$ Ref. [200]
$\pi^0(+\eta)$	0.206	0.0459	0.0279	0.039
π^+	0.206	0.0489	0.0302	0.046
π^-	0.156	0.0324	0.0191	0.033
K^+	0.030	0.0071	0.0044	0.0090
K^-	0.018	0.0036	0.0021	0.0028
$K_L + K_S$	0.043	0.0092	0.0054	–
$p + \bar{p}$	0.217	0.126	0.107	0.263
$n + \bar{n}$	0.114	0.052	0.040	0.035

Index	$\gamma = 1.7$			
Sibyll 2.3 [155]	p - p	p -air	π^+ -air	K^+ -air
$\pi^0(+\eta)$	0.035	0.039	0.054	0.042
π^+	0.041	0.040	0.206	0.058
π^-	0.25	0.026	0.043	0.033
K^+	0.0088	0.0083	0.012	0.135
K^-	0.0024	0.0026	0.0061	0.0055
$K_L + K_S$	0.0087	0.0088	0.0018	0.064
$p + \bar{p}$	0.253	0.185	0.0096	0.011
$n + \bar{n}$	0.089	0.077	0.011	0.0084

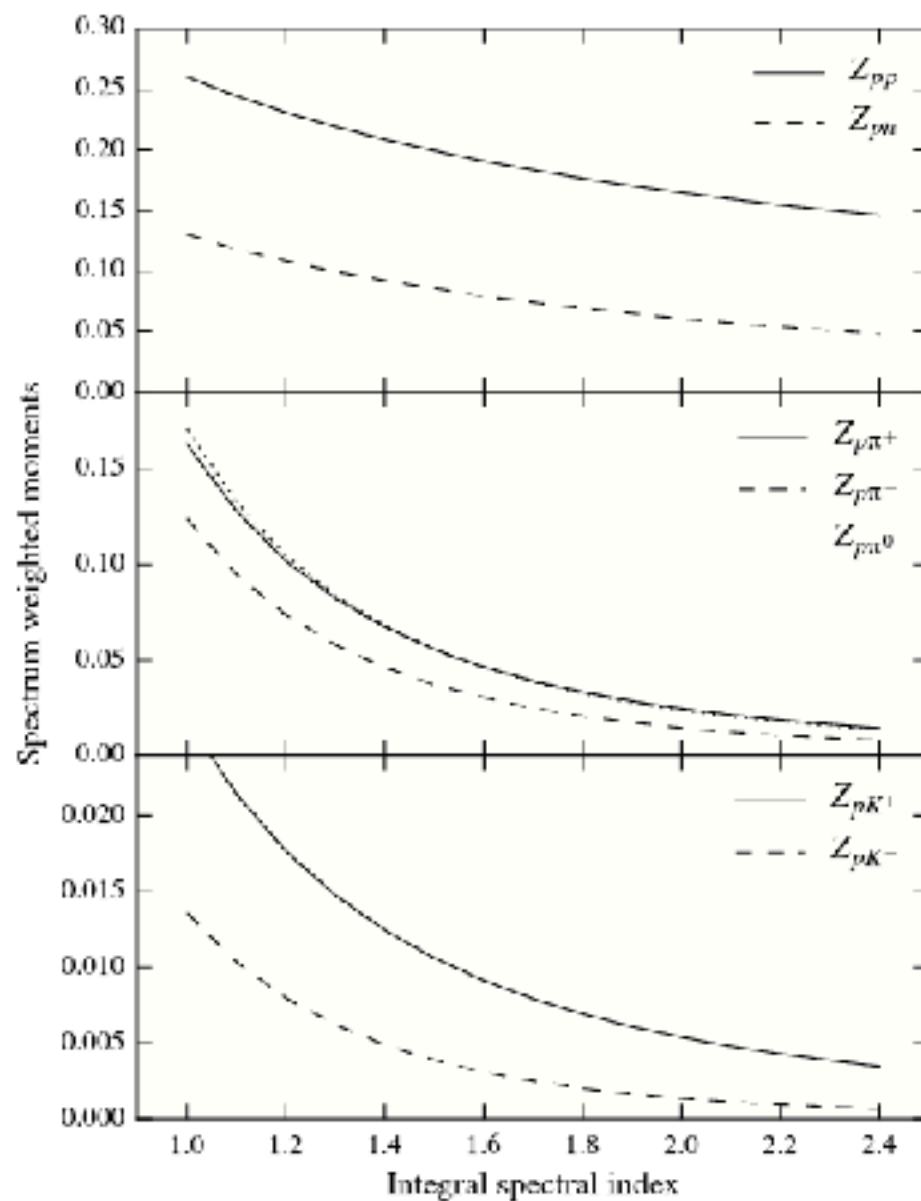


Figure 5.2 Spectrum-weighted moments calculated with Sibyll 2.3 [155]. Shown is the dependence on the integral index of the power law of the primary protons interacting with air at 1 TeV.

5.5.2 Fluxes of neutrons and protons

Eq. 5.46 gives the total flux of neutrons plus protons. The corresponding solutions for n and p separately depend on the four moments

$$Z_{pp} = Z_{nn} \quad \text{and} \quad Z_{pn} = Z_{np}. \quad (5.49)$$

These two independent parameters can be expressed in terms of two independent attenuation lengths:

$$\Lambda_+ = \Lambda_N \equiv \lambda_N(1 - Z_{NN})^{-1} \quad \text{and} \quad \Lambda_- \equiv \lambda_N(1 - Z_{pp} + Z_{pn})^{-1}, \quad (5.50)$$

where $Z_{NN} = Z_{pp} + Z_{pn}$. In Approximation Λ , the ratio of neutrons to protons is

$$\frac{n(X)}{p(X)} = \frac{1 - \delta_0 \exp(-X/\Lambda^*)}{1 + \delta_0 \exp(-X/\Lambda^*)}. \quad (5.51)$$

Here $\delta_0 \equiv (p_0 - n_0)/(p_0 + n_0)$ is the relative proton excess at the top of the atmosphere and $\Lambda^* \equiv (\Lambda_+ - \Lambda_-)/(\Lambda_+ \Lambda_-)$. Eq. 5.51 is derived by writing coupled equations for neutrons and protons and solving them for $n(E, X)$ and $p(E, X)$ in Approximation Λ , neglecting production of $N\bar{N}$ pairs.

5.6 Hadrons in the atmosphere

Since all types of hadrons can be produced when an energetic hadron of any flavor interacts, the set of coupled transport equations represented by Eq. 5.1 is needed to describe hadron fluxes in the atmosphere in more detail.

A direct way to handle a detailed treatment of particle fluxes is with a Monte Carlo simulation or a numerical integration of the transport equations. A study of analytic solutions is useful for qualitative understanding and to check numerical results. We will also use the analytic forms in Chapter 6 to derive approximate formulas for the fluxes of atmospheric muons and neutrinos.

For this purpose it is sufficient to look at Eq. 5.1 in the pion–nucleon and kaon–nucleon sectors, neglecting nucleon–antinucleon production as well as the coupling between pions and kaons and the couplings to other channels. Then we have to consider only Eq. 5.40 together with a simplified equation for the pion fluxes of pions and kaons. For example, for the sum of π^+ and π^- we can write

$$\frac{d\Pi}{dX} = -\left(\frac{1}{\lambda_\pi} + \frac{1}{d_\pi}\right)\Pi + \int_0^1 \frac{\Pi(E/x_L) F_{\pi\pi}(E_\pi, E_\pi/x_L)}{\lambda_\pi(E/x_L)} \frac{dx_L}{x_L^2} + \int_0^1 \frac{N(E/x_L) F_{N\pi}(E_\pi, E_\pi/x_L)}{\lambda_N(E/x_L)} \frac{dx_L}{x_L^2}. \quad (5.52)$$

interaction decay

The equation for kaons has the same form. The decay length is obtained from Eq. 5.3.

5.7 The atmosphere

The relation between altitude and depth is shown in Figure 5.1. X is the slant depth along the trajectory of a high-energy particle entering the atmosphere with zenith angle θ as seen from the ground. The cascade of particles develops along the direction of the vector \vec{X} , and θ^* is the local zenith angle at a point along the trajectory at altitude h . In general, $\theta^* < \theta$ because of the curvature of the Earth. For angles not too large ($\theta < 65^\circ$), the flat Earth approximation can be used, and the distance to the point at h is $\ell = h / \cos \theta$.

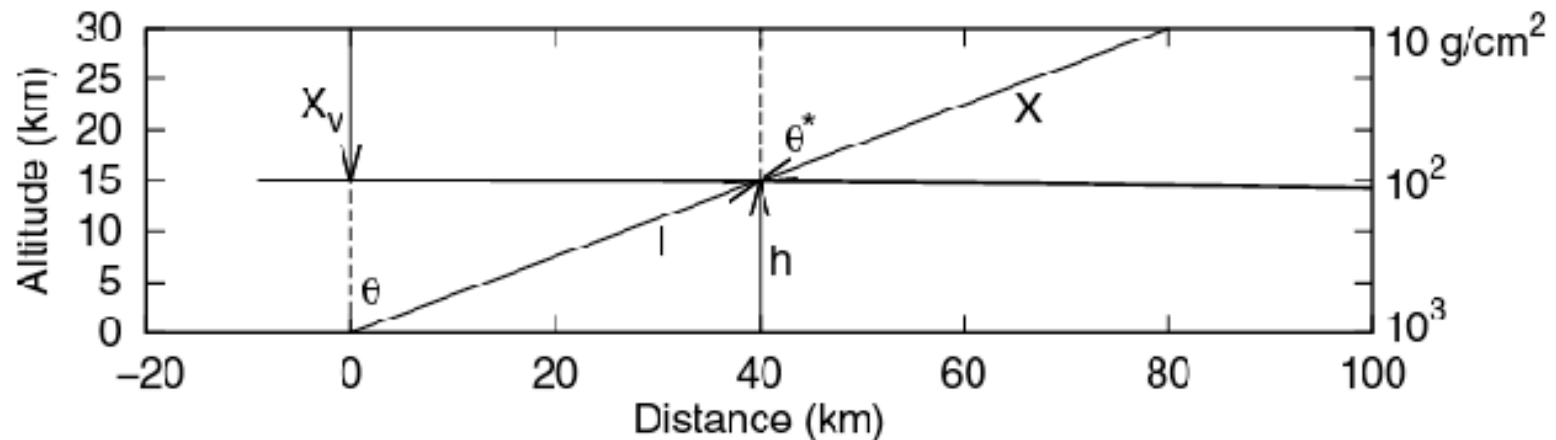


Figure 5.1 Definition of variables to describe the atmosphere. X is the slant depth, θ^* is the local zenith angle in the atmosphere at slant depth X , and h is the local vertical altitude. Vertical depth (g/cm^2) is indicated on the right. The zenith angle θ at the detector is larger than θ^* because of curvature of the Earth.

5.7 The atmosphere

The relation between altitude and depth is shown in Figure 5.1. X is the slant depth along the trajectory of a high-energy particle entering the atmosphere with zenith angle θ as seen from the ground. The cascade of particles develops along the direction of the vector \vec{X} , and θ^* is the local zenith angle at a point along the trajectory at altitude h . In general, $\theta^* < \theta$ because of the curvature of the Earth. For angles not too large ($\theta < 65^\circ$), the flat Earth approximation can be used, and the distance to the point at h is $\ell = h / \cos \theta$.

In general, the relation between vertical altitude (h) and distance up the trajectory (ℓ) is (for $\ell/R_\oplus \ll 1$)

$$h \cong \ell \cos \theta + \frac{1}{2} \frac{\ell^2}{R_\oplus} \sin^2 \theta, \quad (5.53)$$

where R_\oplus is the radius of the Earth. The corresponding slant depth is

$$X = \int_\ell^\infty \rho \left[h = \ell \cos \theta + \frac{1}{2} \frac{\ell^2}{R_\oplus} \sin^2 \theta \right] d\ell. \quad (5.54)$$

The pressure at vertical depth X_v in the atmosphere is $P = gX_v$, where g is the gravitational constant. The density is $\rho = -dX_v/dh$. Thus

$$\frac{gX_v}{-dX_v/dh} = \frac{P}{\rho} = \frac{RT}{M}, \quad (5.55)$$

where the last step follows from the ideal gas law. For dry air with 78.09% nitrogen, 20.95% oxygen and 0.93% argon, $M = 0.028964$ kg/mol. Rewriting Eq. 5.55 as

$$\frac{d \ln(X_v)}{dh} = -\frac{Mg}{RT} \quad (5.56)$$

leads to an exponential solution for an isothermal atmosphere

$$X_v = X_0 e^{-h/h_0}, \quad (5.57)$$

with a scale height

$$h_0 = \frac{RT}{Mg} = 29.62 \text{ m/K} \times T. \quad (5.58)$$

For example, for a typical temperature in the lower stratosphere of 220 K, the scale height is ≈ 6.5 km. At sea level the total vertical atmospheric depth is $X_0 \cong 1030 \text{ g/cm}^2$.

In reality the temperature and hence the scale height decrease with increasing altitude until the tropopause (12–16 km). At sea level $h_0 \cong 8.4$ km, and for $40 < X_v < 200$ g/cm², where production of secondary particles peaks, $h_0 \cong 6.4$ km. A useful parametrization⁵ of the relation between altitude and vertical depth (due to M. Shibata) is

$$h_v(\text{km}) = \begin{cases} 47.05 - 6.9 \ln X_v + 0.299 \ln^2 \frac{X_v}{10}, & X_v < 25 \text{ g/cm}^2 \\ 45.5 - 6.34 \ln X_v, & 25 < X_v < 230 \text{ g/cm}^2 \\ 44.34 - 11.861(X_v)^{0.19}, & X_v > 230 \text{ g/cm}^2. \end{cases} \quad (5.59)$$

The density and atmospheric depth is tabulated as function of height for the US standard atmosphere [201] in Appendix A.7.

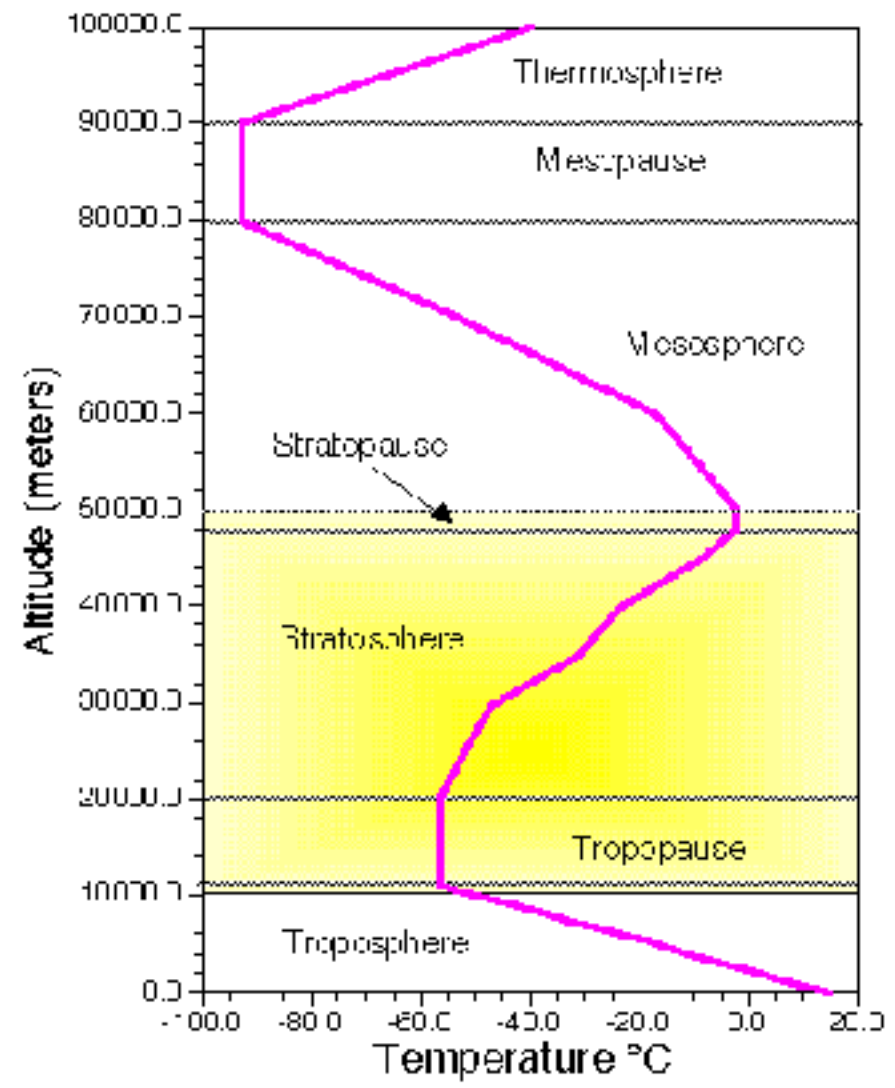
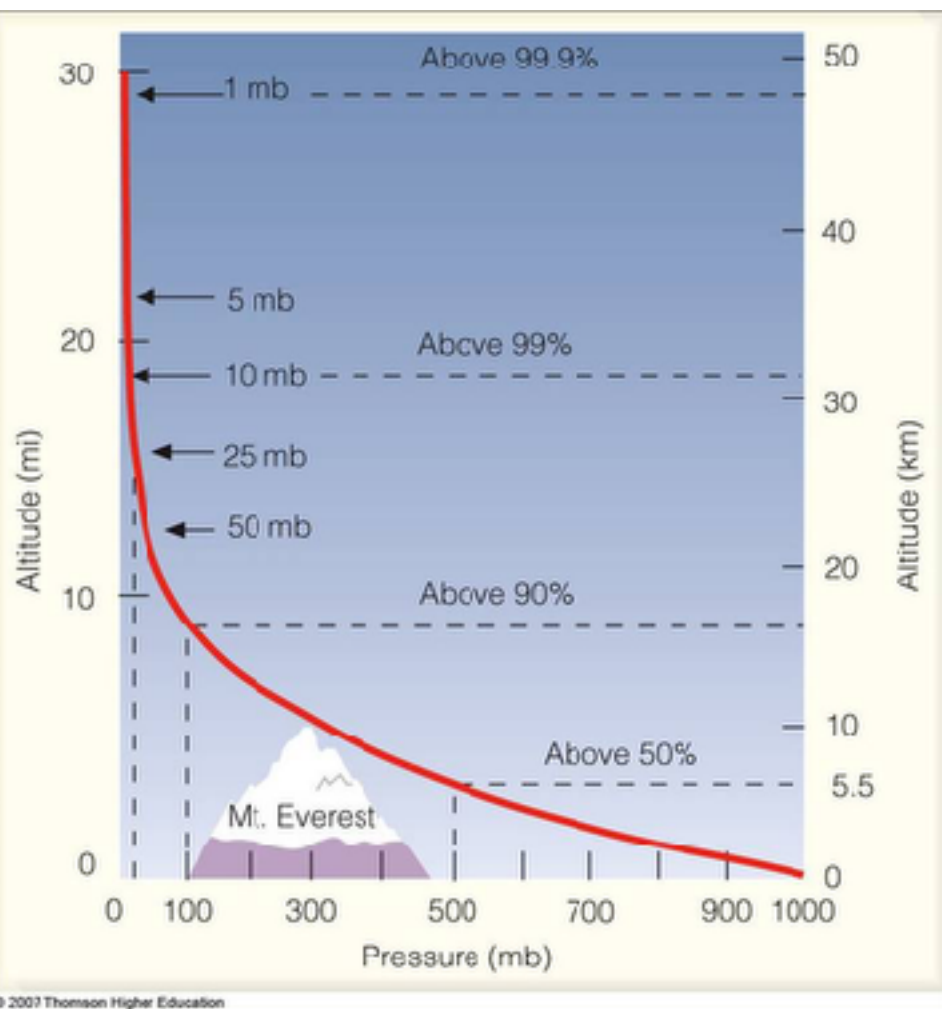
For $\theta \leq 65^\circ$ the second term in Eq. 5.53 can be neglected, and Eq. 5.54 can be evaluated to obtain

$$\rho = \frac{-dX_v}{dh} = \frac{X_v}{h_0} \cong \frac{X \cos \theta}{h_0}, \quad (5.60)$$

with h_0 evaluated at the appropriate atmospheric depth. Then from Eq. 5.3,

$$\frac{1}{d_\pi} = \frac{m_\pi c^2 h_0}{E c \tau_\pi X \cos \theta} = \frac{m_\pi c^2}{E X \cos \theta} \frac{1}{c \tau_\pi} \frac{RT}{Mg} \equiv \frac{\epsilon_\pi}{E X \cos \theta}. \quad (5.61) \text{ decay length}$$

Decay or interaction dominates depending on whether $1/d_\pi$ or $1/\lambda_\pi$ is larger in Eq. 5.52. This in turn depends on the relative size of $\epsilon_\pi/\cos \theta$ and E (assuming $X \approx \lambda_\pi$), and similarly for other particles. Since most particle interactions occur in the first few interaction lengths, we summarize the decay constants for various particles using the high altitude value of $h_0 \cong 6.4$ km in Table 5.3.



Decay or interaction dominates depending on whether $1/d_\pi$ or $1/\lambda_\pi$ is larger in Eq. 5.52. This in turn depends on the relative size of $\epsilon_\pi/\cos\theta$ and E (assuming $X \approx \lambda_\pi$), and similarly for other particles. Since most particle interactions occur in the first few interaction lengths, we summarize the decay constants for various particles using the high altitude value of $h_0 \cong 6.4$ km in Table 5.3.

Table 5.3 *Decay constants for various particles*

Particle	$c\tau$ (cm)	ϵ (GeV)
μ^\pm	6.59×10^4	1.0
π^\pm	780	115
π^0	2.5×10^{-6}	3.5×10^{10}
K^\pm	371	850
K_S	2.68	1.2×10^5
K_L	1534	208
D^\pm	0.031	3.7×10^7
D^0	0.012	9.9×10^7

5.8 Meson fluxes

In the limit that $E \gg \epsilon_\pi$, decay can be neglected. Then the scaling limit solution of Eq. 5.52, subject to the boundary condition $\Pi(E, 0) = 0$, is

$$\Pi(E, X) = N(E, 0) \frac{Z_{N\pi}}{1 - Z_{NN}} \frac{\Lambda_\pi}{\Lambda_\pi - \Lambda_N} \left(e^{-X/\Lambda_\pi} - e^{-X/\Lambda_N} \right). \quad (5.62)$$

The moments Z_{ac} are defined in Eq. 5.48, and the attenuation lengths are related to the interaction lengths by

$$\Lambda_l \equiv \lambda_l (1 - Z_{ll})^{-1} \quad (5.63)$$

The solution for charged kaons is the same as for charged pions with subscript π replaced by subscript K . Interaction and attenuation lengths in the atmosphere are given in Table 5.4, based on cross sections and Z-factors of Sibyll 2.3 [155], see

Table 5.4 *Atmospheric interaction and attenuation lengths for $\gamma = 1.7$ in air, in units of g/cm^2 . The values are calculated with Sibyll 2.3 [155].*

E_{lab} (GeV)	λ_N	Λ_N	λ_π	Λ_π	λ_K	Λ_K
100	88	120	116	155	134	160
1000	85	115	111	148	122	147
10000	79	106	101	135	110	133
100000	72	97	87	114	95	114

5.8 Meson fluxes

In the limit that $E \gg \epsilon_\pi$, decay can be neglected. Then the scaling limit solution of Eq. 5.52, subject to the boundary condition $\Pi(E, 0) = 0$, is

$$\Pi(E, X) = N(E, 0) \frac{Z_{N\pi}}{1 - Z_{NN}} \frac{\Lambda_\pi}{\Lambda_\pi - \Lambda_N} \left(e^{-X/\Lambda_\pi} - e^{-X/\Lambda_N} \right). \quad (5.62)$$

The moments Z_{ac} are defined in Eq. 5.48, and the attenuation lengths are related to the interaction lengths by

$$\Lambda_l \equiv \lambda_l (1 - Z_{ll})^{-1} \quad (5.63)$$

The solution for charged kaons is the same as for charged pions with subscript π replaced by subscript K . Interaction and attenuation lengths in the atmosphere are given in Table 5.4, based on cross sections and Z-factors of Sibyll 2.3 [155], see also Table 5.2. The pion flux given by Eq. 5.62 rises from zero at the top of the atmosphere to a maximum at

$$X = \ln(\Lambda_\pi/\Lambda_N) \times (\Lambda_N \Lambda_\pi)/(\Lambda_\pi - \Lambda_N) \sim 140 \text{ g/cm}^2. \quad (5.64)$$

It then declines, eventually with attenuation length Λ_π . This behavior is characteristic of secondary fluxes in the atmosphere when decay can be neglected.

Before going on to consider the solutions at lower energy, where decay is important, it is instructive to consider the sum of all hadrons at high energy. Within the simplified coupling scheme we are using, the total flux of hadrons is

$$\Sigma = N(E, 0) \left[e^{-X/\Lambda_N} + \frac{Z_{N\pi}}{1 - Z_{NN}} \frac{\Lambda_\pi}{\Lambda_\pi - \Lambda_N} \left(e^{-X/\Lambda_\pi} - e^{-X/\Lambda_N} \right) + \frac{Z_{NK}}{1 - Z_{NN}} \frac{\Lambda_K}{\Lambda_K - \Lambda_N} \left(e^{-X/\Lambda_K} - e^{-X/\Lambda_N} \right) \right]. \quad (5.65)$$

Let us now consider Eq. 5.65 for a very flat spectrum, $\gamma = 1$. This corresponds to the *normal solution* in electromagnetic cascade theory. Let us further artificially treat the π^0 as stable instead of feeding its electromagnetic component via $\pi^0 \rightarrow \gamma\gamma$. Then by energy conservation $Z_{\pi\pi}(\gamma = 1) = 1$. Also, since in this artificial example we neglect $K \rightarrow \pi$ and $K \rightarrow N$, $Z_{KK} = 1$ and $Z_{NN} + Z_{N\pi} + Z_{NK} = 1$. Thus the expression in square brackets in Eq. 5.65 is 1, so an incident spectrum with $\gamma = 1$ preserves itself without attenuation. Note, however, that this requires infinite energy: the energy contained in a spectrum is

$$\int E \left| \frac{dN}{dE} \right| dE \propto \int E \left[E^{-(\gamma+1)} \right] dE, \quad (5.66)$$

which is logarithmically divergent for $\gamma = 1$.

Returning now to the real world, we consider the transport equation for charged pions at lower energy, where pion decay cannot be neglected. Then the scaling version of Eq. 5.52 is

$$\begin{aligned}
 d\Pi/dX = & - \left(\frac{1}{\lambda_\pi} + \frac{\epsilon_\pi}{E X \cos\theta} \right) \Pi(E, X) \\
 & + \frac{1}{\lambda_\pi} \int_0^1 \Pi(E/x_L, X) F_{\pi\pi}(x_L) \frac{dx_L}{x_L^2} \\
 & + \frac{Z_{N\pi}}{\lambda_N} N(E, 0) e^{-X/\Lambda_N}.
 \end{aligned}
 \tag{5.67}$$

An explicit approximate expression for the solution can be found if $\Pi(E, X)$ is replaced under the integral in Eq. 5.67 by a factorized form which is a product of $E^{-(\gamma+1)}$ and a function of depth. The motivation for this trial form is that the driving source term in Eq. 5.67 is proportional to the nucleon flux, which has the $E^{-(\gamma+1)}$ dependence on energy.

With this *ansatz* Eq. 5.67 becomes

$$\frac{d\Pi}{dX} = -\Pi(E, X) \left(\frac{1}{\Lambda_\pi} + \frac{\epsilon_\pi}{E X \cos\theta} \right) + \frac{Z_{N\pi}}{\lambda_N} N_0(E) e^{-X/\Lambda_N}. \quad (5.68)$$

The effect of this approximation is to represent the pion interaction and regeneration in Eq. 5.67 by a single attenuation term with attenuation length Λ_π . The last term in Eq. 5.68 is the production spectrum of pions by nucleons. The exact solution of Eq. 5.68 is

$$\Pi(E, X) = e^{-(X/\Lambda_\pi)} \frac{Z_{N\pi}}{\lambda_N} N_0(E) \int_0^X \exp \left[\frac{X'}{\Lambda_\pi} - \frac{X'}{\Lambda_N} \right] \left(\frac{X'}{X} \right)^{\epsilon_\pi/E \cos\theta} dX'. \quad (5.69)$$

In the high-energy limit $(X'/X)^{\epsilon_\pi/E \cos\theta} \rightarrow 1$ Eq. 5.69 reduces to Eq. 5.62. In the low-energy limit $E \cos\theta \ll \epsilon_\pi$, so $(X'/X)^{\epsilon_\pi/E \cos\theta}$ is small except for X' near X . In this low-energy limit therefore one can set $X' = X$ in the exponential and Eq. 5.69 becomes

$$\Pi(E, X) \xrightarrow{E \ll \epsilon_\pi} \frac{Z_{N\pi}}{\lambda_N} N(E, 0) e^{-X/\Lambda_N} \frac{X E \cos\theta}{\epsilon_\pi}. \quad (5.70)$$